*34th EPS Conference on Plasma Phys. Warsaw, 2 - 6 July 2007 ECA Vol.**31F**, P-4.125 (2007)*

Analysis of pressure profiles and transport simulations of MAST and JET discharges

Yu.N. Dnestrovskij[1], J.W. Connor[2], S.V. Cherkasov[1], A.V. Danilov[1], A.Yu. Dnestrovskij[1], N.A. Kirneva[1], S.E. Lysenko[1], C.M. Roach[2], M. Walsh[2] and JET-EFDA contributors

[1] *Nuclear Fusion Institute, RRC 'Kurchatov Institute', 123182 Moscow, Russia*
[2] *EURATOM-UKAEA Fusion Association, Culham Science Centre, Abingdon, Oxon, UK*

1. Introduction

It is well known that the temperature profiles in a tokamak are self-consistent [1-2]. This feature allows one to construct the heat conductivity equation in terms of so called "critical temperature gradients" [3-5]. In our previous works this critical gradient is expressed through the gradient of the canonical temperature profile [6, 7]. The concept of pressure profile conservation has attracted so far much less attention. Recently in [8] we analysed the pressure profiles from several devices. In this report we continue this work using for the analysis the larger set of MAST shots. As a result we construct the particle flux similarly to the heat flux in previous model [6,7,8]. The proposed transport model, which includes both the heat and particle transport equations, is used to simulate the set of MAST shots. We provide also the simulation of a series of JET shots by two different models. The first one based on the "critical temperature gradient" ideas, includes the energy balance only. This allows us to compare the results obtained by our model with results obtained by other models [9]. The second one is the full version of the CPTM model, which includes both the energy and particle balances.

2. Main points of the CPTM

The heat and particle fluxes, q_α (α = e, i) and Γ, are described by the expressions

$$q_\alpha = -n\chi_\alpha^{PC} T_\alpha \left(T_\alpha'/T_\alpha - T_c'/T_c\right) H\left(-[T_\alpha'/T_\alpha - T_c'/T_c]\right) - n\chi_\alpha^{0} T_\alpha' + 3/2\,\Gamma T_\alpha - n\chi_\alpha^{MHD} T_\alpha' \quad (1)$$

$$\Gamma = -D\,n\,(p_e'/p_e - p_c'/p_c) - D^{MHD} n' + \Gamma^{neo}, \quad (2)$$

where T_α and n are the temperatures and density to be determined, T_c and p_c are the canonical profiles of temperature and pressure, χ_α^{PC} and D are stiffness coefficients (in m^2/s) for temperature and pressure profiles, $\Gamma^{neo} = n\,v^{neo}$, $H(x)$ is the Heaviside function, χ_α^{MHD} and D^{MHD} simulate sawtooth mixing. The electron pressure $p_e = nT_e$ instead of total pressure $p = p_e + p_i$ is used in (2) for simplicity. We set in this Report

$$D = C_n \chi_e^{PC}, \quad C_n = 0.08 \quad (3)$$

This value of C_n leads to a reasonable value of the required cold neutrals influx Q_N in the range $Q_N = (2 - 10)\times10^{21}$ s^{-1}, depending on plasma density and deposited power. The low value of C_n (C_n<<1) means that the stiffness of the pressure profile (from the point of view of the model) is much less than the stiffness of the temperature profile. The absolute values of χ_α^{PC} were found by the comparison of calculations with experiment [7, 10]:

$$\chi_\alpha^{PC} = C_{T\alpha}\,(1/M)\,(a/R)^{0.75} q(\rho = \rho_{max}/2) q_{cyl}\,(T_e(\rho = \rho_{max}/4))^{1/2}\,(3/R)^{1/4}\,(1/B_0)\,n_{av}/n \quad (4)$$

Here T_α [keV], B_0 [T], R and a [m], n_{av} is the line-averaged density [10^{19} m^{-3}], $C_{Te} = 3.5$, $C_{Ti} = 5$. The values of χ_α^{0} are several times less than χ_α^{PC}, and they play the essential role only for the off-axis heating. For χ_α^{0} we use the expression $\chi_\alpha^{0} = C_0\,(T_\alpha)^{1/2}\,n_{av}/(nR)$, where C_0 = 1-2.

The canonical profile of $\mu_c = 1/q_c$ satisfies the following boundary problem [6]

$$\rho^2 G\,\partial\mu^2/\partial\rho + \lambda/2\,\partial/\partial\rho\,((1/V')\,\partial/\partial\rho\,(V' G\rho\mu)) + C\rho\mu'/V' = 0 \quad (5)$$

$$\mu(0) = \mu_0 > 0, \quad \mu'(0) = 0, \qquad \mu(\rho_{max}) = \mu_a, \quad (\mu_0/2)\{\,i/[G\,\mu^2]\}(\rho=\rho_{max}) = U \quad (6)$$

where λ and C are the Lagrange multipliers, V' and G are the metric coefficients, μ_a is defined by the solution of the Grad-Shafranov equilibrium equation, $U \sim 1$ is a constant defined by the condition

$$\partial Z(\rho)/\partial\rho\ (\rho = \rho_{max}) = 0, \qquad (7)$$

where $Z(\rho) = (\mu_0/2)\ i_c(\rho)/[G(\rho)\ \mu_c(\rho)^2]$, $i_c(\rho) = (1/V')\ \partial/\partial\rho\ (V'G\rho\mu_c)$ is the dimensionless canonical current density. We propose also that $p_c \sim i_c$ and $T_c'/T_c = 2/3\ p_c'/p_c$ [3, 11].

3. Simulation of MAST discharges

To analyze the experimental pressure profiles several groups of MAST shots were considered: two Ohmic (OH) shots (##12301, 12303) with current $I = 0.7$ MA and densities $n_{av} = 3.4$ and 4.7×10^{19} m^{-3}; one OH shot (#12331) with $I = 0.52$ MA, $n_{av} = 0.85\times10^{19}$ m^{-3}; two NBI shots (##9003, 9005) with $I = 0.7$ MA, high densities $n_{av} = 5.5$ and 5.0×10^{19} m^{-3} and deposited NBI power $P_{NB} = 1.2$ and 0.85 MW; six NBI shots with $I = 0.75$ MA, $n_{av} = (1.6–3.6)\times10^{19}$ m^{-3}, deposited power $P_{NB} = 1.1 – 1.6$ MW. In figure 1 the relative pressure gradients of the last group of shots are shown. This series imitates the evolution of the particular discharge. It is seen that the profiles are close to each other in the gradient region. It confirms the conservation of pressure profiles in the gradient region during the discharge evolution. The analysis of other shots confirms also such a conclusion.

There are sawtooth oscillations for all MAST shots, so we choose $\mu_0 = 1.2$-1.3, which corresponds to the $\mu_c = 1$ surfaces lying close to the experimental ones. The example of the simulation of two NBI shots by the CPTM is shown in figure 2. We introduce the off-set linear and quadratic RMS deviations to compare the experimental and calculated temperatures:

$$\mathrm{d1}T = (1/N)\sum_k^N \frac{T_k^{calc} - T_k^{exp}}{T_k^{exp}} \qquad \mathrm{d2}T = \{(1/N)\sum_k^N [\frac{T_k^{calc} - T_k^{exp}}{T_k^{exp}}]^2\}^{1/2} \qquad (8)$$

and the similar values for plasma density. The index k marks the experimental points in space. Note that for MAST the summation is produced only over points placed outside the MHD mixing region. The results of the simulation are shown in figure 3 a,b. Here the linear (a) and RMS (b) deviations of the electron temperature and density are shown for all 11 shots described above. It is seen that the linear deviations are less than 10-12%. The RMS deviations are several times larger than linear ones. It can be explained by the rather large scatter of the experimental points and by the small shift of the calculated profiles from the experimental ones that is seen in figure 2.

4. Simulation of JET discharges

Ten JET ELMy H-mode shots were chosen for simulation [9]. The main parameters of these shots and some calculation results are shown in Table. The first (Reduced) model with energy balance only includes the heat fluxes (1) for electrons and ions. The linear deviations for the electron and ion temperatures are shown in figure 4; the RMS deviations for the electron temperature ($\mathrm{d2}T_eR$) are included in Table. The calculation results in figure 4 are plotted versus plasma current I. The simulation of JET shots with the full version of the CPTM was carried out also. The RMS deviations for the electron and ion temperatures (red and green) and plasma density (blue) are shown in figure 5. It is seen that the deviations for density do not exceed 10-12%. The RMS deviations for the electron temperature ($\mathrm{d2}T_eF$) and density ($\mathrm{d2}n$) are also included in Table. The deviations really depend on the choice of the parameter μ_0, which we set to an "optimal" value $\mu_0^{opt} = (3.5 – 4)/q_a = (3.5 – 4)\ \mu_a$. The calculations have shown that in the vicinity of μ_0^{opt} there is a wide enough range of μ_0, where all deviations change slowly.

In figure 6 we compare the experimental and calculated values of $R/L_{Te} = -(T_e'/T_e)$ (a) and $R/L_p = -R(p'/p)$ (b) at the point $\rho = 0.5$ ($p = p_e + p_i$). The calculated relative gradients of

canonical profiles R/L_{Tc} and R/L_{pc} are shown also. The experimental values shown are really averaged over the time-interval Δt = 0.6 – 2 s. The error bars are determined by the time behaviour of these values. The calculated values of R/L_{Te} and R/L_p are very close to the experimental ones. Note that there are some shots with large space and time oscillations of temperature and pressure profiles in the vicinity of resonant surfaces, for which the experimental points in figure 6 are not shown. Such shots are marked in figure 6. The distances $\Delta_T = R/L_{Te} - R/L_{Tc}$ and $\Delta_p = R/L_p - R/L_{pc}$ are included in fluxes (1-2). It is seen from figure 6a that Δ_T is low for currents larger than 2.4 MA. For these shots the values of q_a are approximately the same, but the plasma density rises with current increase. So the stiffness of temperature profiles rises also and the values of Δ_T diminish. We do not observe such dependences in the behaviour of Δ_p and this corresponds with low value of C_n.

Hence, in this report we propose the transport model (1-2) based on the ideas of canonical profiles and formulated in terms of critical gradients for electron and ion temperatures and pressure. The simulations done so far have shown that the model can produce reasonable results. These initial tests motivate further work to broaden the database for the successful application of this model, in particular by considering cases of extreme variations of density profiles peakedness, such as observed in JET H-mode plasmas for increasing collisionality.

Acknowledgments

Authors thank Dr. P. Mantica and Dr. I. Voitsekhovitch for helpful discussions. The work is supported by Rosatom, by Contract 02.516.11.6068 and by UKAEA Consultancy Agreement No 3000080910.

References

[1] B. Coppi, Comments Plasma Phys. Control. Fusion 5, 261 (1980)
[2] Yu.V. Esiptchuk and K.A. Razumova, Plasma Phys. Control. Fusion 28, 1253 (1986)
[3] Yu.N. Dnestrovskij and G.V. Pereverzev, Plasma Phys. Control. Fusion 30, 47 (1988)
[4] P.H. Rebut, P.P. Lallia and M.L. Watkins, in Plasma Phys. and Controlled Nuclear Fusion Research, IAEA, Vienna, 2, 191 (1989)
[5] F. Ryter et al., Plasma Phys. Control. Fusion 43, A323 (2001)
[6] Yu.N. Dnestrovskij et al., Plasma Phys. Rep. 28, 887 (2002)
[7] Yu.N. Dnestrovskij, A.Yu. Dnestrovskij and S.E. Lysenko, Plasma Phys. Rep. 31, 529 (2005)
[8] Yu.N. Dnestrovskij et al., Nucl. Fusion 46, 953 (2006)
[9] Voitsekhovitch I. et al., 33-rd EPS Conf, Rome, ECA, 30I, P-1.078 (2006)
[10] Yu.N. Dnestrovskij et al., Nucl. Fusion 35, 1047 (1995)
[11] E. Minardi, Phys. Letts. A 240, 70 (1998)

Table. Parameters of JET shots and some results of calculations.

	#shot	I, MA	n_{av}, 10^{19} m^{-3}	P_{NB}, MW	q_a	d2T_eR	d2T_eF	D2n
1	61103	2.75	6.4	15	3.13	0.12	0.08	0.14
2	61138	2.5	8.25	14	3.66	0.08	0.15	0.09
3	61174	2.35	5.6	12	2.91	0.07	0.08	0.06
4	61132	2.35	2.3	2.5	3.16	0.06	0.12	0.12
5	61097	2	4.8	8	2.96	0.05	0.07	0.08
6	61366	1.5	2.9	14	4.27	0.2	0.15	0.03
7	61543	1.5	4.14	14	4.52	0.1	0.11	0.08
8	61520	1.4	3.1	14	6.3	0.18	0.18	0.05
9	61526	1	2.4	7.9	6.3	0.12	0.17	0.08
10	61236	1	2.3	12.5	11	0.18	0.14	0.12

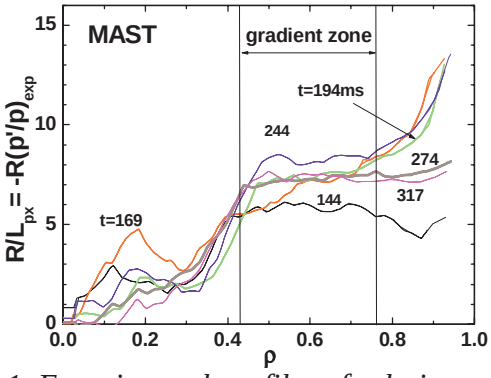

Fig. 1. Experimental profiles of relative pressure gradient at different time instants.

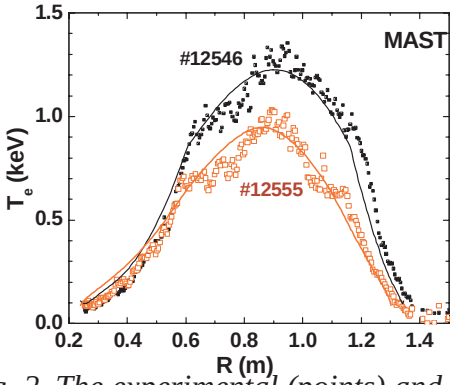

Fig. 2. The experimental (points) and predicted by CPTM (lines) electron temperature profiles for NBI MAST shots.

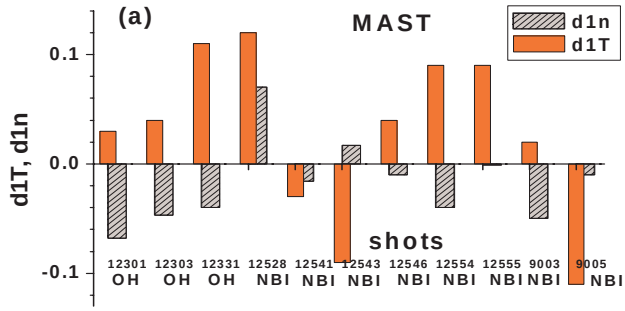

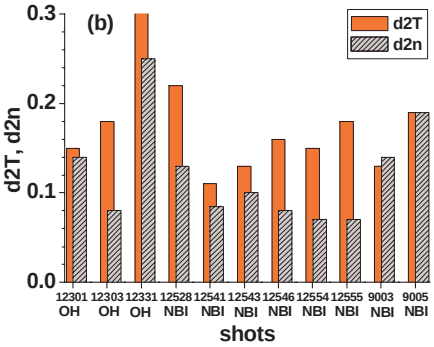

Fig. 3. Linear (a) and RMS (b) deviations of calculated density and temperature profiles from experimental ones for MAST.

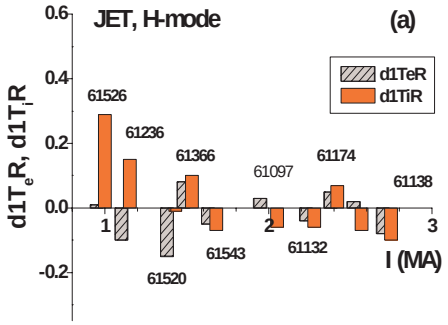

Fig. 4. Linear deviations of calculated temperature profiles from experimental ones obtained by reduced version of the CPTM.

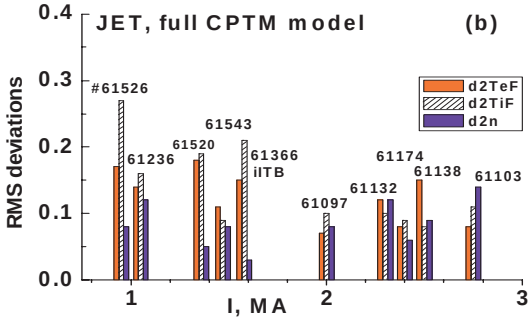

Fig. 5. RMS deviations for temperatures and density obtained by full version of the CPTM.

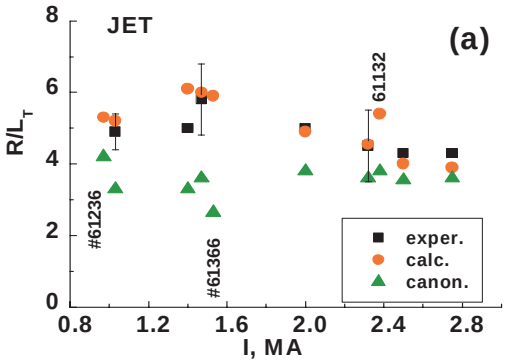

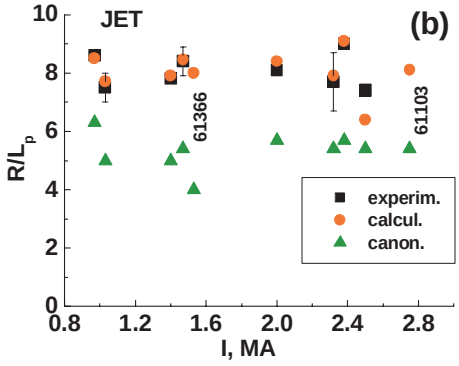

Fig.6. The experimental, calculated and canonical values of relative gradients for temperature (a) and pressure (b) for chosen JET shots at ρ=0.5. Error bars are obtained during time averaging. For marked shots the experimental values of R/L_T and R/L_p are unavailable due to profile gradient uncertainties.